



ORIGINAL ARTICLE

Highly efficient persulfate oxidation process activated with Fe⁰ aggregate for decolorization of reactive azo dye Remazol Golden Yellow



Chih-Huang Weng ^{*}, Hong Tao

Department of Civil and Ecological Engineering, I-Shou University, Da-Shu District, Kaohsiung City 84008, Taiwan

Received 15 November 2014; accepted 16 May 2015

Available online 3 June 2015

KEYWORDS

Decolorization;
Persulfate oxidation;
Reactive dye;
Remazol Golden Yellow;
Wastewater treatment;
Zero-valent iron

Abstract The commercially available Fe⁰ aggregate has advantages of low-cost, fast-effective decontamination, reusability, and ease of operation. However, little study has been done on the performance of Fe⁰ aggregate as a catalyst in degradation of azo dyes, particularly used in persulfate (PS) oxidation process. This study investigated decolorization of a reactive azo dye, Remazol Golden Yellow (RGY, Reactive Orange 107), by persulfate oxidation activated with Fe⁰ aggregate. RGY decolorization was not effective in ultrasound-activated, heat-activated, and base-activated persulfate oxidation; however, a significant decolorization improvement was achieved by applying Fe⁰ aggregate to activated persulfate (PS/Fe⁰). Decolorization was strongly influenced by pH, Fe⁰, persulfate dosages and temperature. The suitable conditions for RGY decolorization were pH 6.0, PS 5×10^{-3} M, and Fe⁰ 0.5 g/L. This condition yields 98% color removal of 100 mg/L RGY solution within 20 min treatment; the azo bonds of RGY were completely broken down. RGY decolorization followed the first-order kinetics. Activation energy of the PS/Fe⁰ system was 0.479 kJ/mol, suggesting the temperature dependence of RGY decolorization is small. The presence of inorganic salt in RGY solution had an adverse effect on decolorization. The inhibitory effect of various inorganic salts on decolorization followed the sequence of Na₂HPO₄ ≫ NaHCO₃ ≫ NaClO₄ > NaCl > NaNO₃ > NaClO₄ > no salt. The Fe⁰ aggregate was reusable and a satisfactory decolorization efficiency was achieved with the repeated use of Fe⁰ for five times. The PS/Fe⁰ process provides an efficiency and effective technology for RGY decolorization.

© 2015 The Authors. Production and hosting by Elsevier B.V. on behalf of King Saud University. This is an open access article under the CC BY-NC-ND license (<http://creativecommons.org/licenses/by-nc-nd/4.0/>).

^{*} Corresponding author. Tel.: +886 929552662; fax: +886 76577461.

E-mail address: chweng@isu.edu.tw (C.-H. Weng).

Peer review under responsibility of King Saud University.



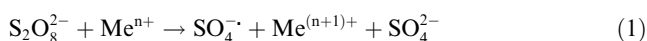
Production and hosting by Elsevier

1. Introduction

Azo dyes, possessing a primary aromatic amino group, are the major colorants used in textile dyeing and printing industries. The effluents released from these industries are highly colored from the use of various dyes. If this effluent is treated inappropriately, it can cause adverse effects on aquatic environments.

Most azo dyes are refractory to biodegradation due to their complex structure and the stability. Thus, dye effluent treated by conventional biological treatment process may no longer meet stringent effluent discharge criteria. A broad range of physico-chemical decolorization methods are currently available, such as adsorption (Somasekhara Reddy and Nirmala, 2014; Pei et al., 2015; Ozbay and Yargic, 2015), membrane separation (Xing et al., 2012), sonophotocatalytic technique (Hemapriyamvadhya and Sivasankar, 2015; Rasalingam et al., 2015), and electrochemical methods (Kobyta et al., 2003; Raschitor et al., 2014); however, chemical sludge generation, adsorbent regeneration, and maintenance of fouled membranes may raise serious concerns (Pukdee-Asa et al., 2011; Weng et al., 2013).

Nowadays, persulfate oxidation (PS) has proven to be a promising technique for the removal of refractory organic pollutants (Liang and Lai, 2008; Oh et al., 2010; Li et al., 2013; Al-Shamsi and Thomson, 2013; Fang et al., 2013; Long et al., 2014) and decolorizing textile and printing industry wastewater (Wang et al., 2014; Li et al., 2014a,b; Cai et al., 2014). The PS process is generally associated with strong reactive sulfate radicals, $\text{SO}_4^{\cdot-}$ ($E^\circ = 2.6 \text{ V}$ vs. normal hydrogen electrode (NHE)). The source of $\text{SO}_4^{\cdot-}$ is often from peroxydisulfate ($\text{S}_2\text{O}_8^{2-}$, PS, $E^\circ = 2.01 \text{ V}$ vs. NHE), which is a strong and stable oxidizing agent and it has high aqueous solubility and high stability at room temperature as compared to hydrogen peroxide (H_2O_2 , $E^\circ = 1.77 \text{ V}$ vs. NHE) (Lin et al., 2013). $\text{SO}_4^{\cdot-}$ can be generated in the reaction mixture by transition metals (Me^{n+}) reactive with persulfate anions ($\text{S}_2\text{O}_8^{2-}$).



$\text{SO}_4^{\cdot-}$ can also be generated through ultraviolet light, thermal energy, microwave, ultrasound, and strong basic solution (Yang et al., 2009; Furman et al., 2010; Xie et al., 2012; Lee et al., 2013; Ji et al., 2015).



where))) refers to the application of ultrasound.



Because Fe is relatively nontoxic and inexpensive among various transition metal catalysts, it has been widely studied to activate persulfate oxidation for contaminant removal. Several types of Fe-based catalysts were used for the chemical activation of persulfate, including nano-sized zero-valent iron (Fe^0) (Wang et al., 2014), biochar supported nano-sized Fe^0 (Yan et al., 2015), zero-valent iron powder (Zhou et al., 2015; Li et al., 2014b), Fe-immobilized resin chars (Shi et al., 2015), Fe oxide-immobilized MnO_2 composite (Jo et al., 2014), Fe_2O_3 (Zhu et al., 2013), ferrous iron (Han et al., 2014), ferrous sulfide ore particles (Yuan et al., 2015), and Fe_3O_4 magnetic nanoparticles (Zhao et al., 2015). Influence of particle size of Fe^0 and comparison of various forms of Fe on the reactivity of activated persulfate oxidation have been studied (Li et al., 2014a; Rodriguez et al., 2014). In the past years, studies have focused on the synthesis of bimetallic-based catalysts and granular activated carbon supported metals as catalyst for heterogeneous activation of peroxydisulfate

(Yang et al., 2011; Su et al., 2013; Lee et al., 2013; Cai et al., 2014). Possible leaching of cobalt from Co-containing catalysts and the high-cost of activated carbon and bimetallic catalysts have raised concerns.

In the PS process, oxidation efficiency is highly depending upon dye type, dye chemical structure, and the operating conditions. Operating conditions must be evaluated before applying any type of activators for persulfate. Reactive dyes is one of the most successful classes of modern synthetic dyes used in textile industry in dyeing wool, silk, cotton, and cellulosic fibers due to their shade versatility, application flexibility, and favorable fastness properties. Commercially available Fe^0 aggregate has long been applied in soil and groundwater remediation for reductive transformation of certain persistent organic and inorganic pollutants (Wilkin et al., 2005; Weng et al., 2007). In this study, an anionic reactive dye, Remazol® Golden Yellow RGB (RGY), a widely used dye in textile processing industries worldwide (Alvarenga et al., 2015) was used as model target compound to evaluate the decolorization efficiency of PS activated with Fe^0 aggregate (PS/Fe^0). To the best of our knowledge, there have been no studies of Fe^0 aggregate as an activator for PS oxidation of reactive dyes. The objectives were to: (a) examine the RGY decolorization efficiency achieved in the PS/Fe^0 system, (b) investigate key operating parameters such as initial pH, Fe^0 and PS dosages, reaction temperature, and salts on the RGY decolorization, and (c) evaluate the reusability of Fe^0 aggregate in the PS/Fe^0 system.

2. Materials and methods

2.1. Materials

RGY (C.I. Reactive Orange 107, $\text{C}_{16}\text{H}_{18}\text{N}_4\text{O}_{10}\text{S}_3\text{Na}_2$), an anionic fiber reactive dye, was obtained from DyStar (Germany) and used as received without further purification. While this sulfonated azo dye is widely used in the textile industry, the biodegradability of this dye is low (<10%). Fe^0 aggregate (Fig. 1) with particle size 0.297–2.380 mm and specific weight 2240–2560 kg/m^3 was obtained from Connelly-GPM (USA). Sodium persulfate ($\text{Na}_2\text{S}_2\text{O}_8$) was purchased from Nippon Shiyaku (Japan). All other reagents were of analytical grade.



Figure 1 Fe^0 aggregate catalyst.

2.2. Persulfate oxidation experiments

Persulfate decolorization experiments were performed in aluminum-foil-wrapped glass beakers containing 1000 mL of RGY solution prepared using distilled water. Unless otherwise stated, the experimental procedures were as follows. (1) The pH of RGY solution was adjusted with 0.01 M HCl/NaOH solution. (2) After adding Fe^0 aggregate and persulfate, RGY solution was immediately agitated with a mechanical stirrer (Shin-kwang, Taiwan) at 800 rpm for 30 min. (3) At preset time intervals, 10 mL of solution was taken by a syringe and filtered immediately through a 0.45- μm membrane filter (Advantec, Japan) to collect the supernatant. We confirmed that the filter and glass beaker could not adsorb the dye. (4) The residual RGY concentration in the supernatant was determined as described in Section 2.3.

The effect of temperature on PS decolorization was investigated under isothermal conditions by maintaining the dye solution in a water circulation bath. The detailed experimental procedures were as described above, except before adding Fe^0 and persulfate [step (2)] the dye solution was placed in the water bath for 0.5 h to reach the designated temperature. In the experiments of PS coupled with sonolysis, the dye solution was sonicated by an ultrasonic generator (S-450A, Branson, USA) equipped with a titanium horn-probe transducer. The sonication was administered in pulses with a 60% duty cycle at 60 kHz and 120 W for 10 min.

Each decolorization experiments were conducted in duplicate, and average values were used in analysis. Decolorization efficiency was calculated as follows:

$$\text{Efficiency (\%)} = (C_o - C_t) / C_o \times 100 \quad (6)$$

where C_o and C_t were the RGY concentration at time 0 and reaction time t (min), respectively. The rate of RGY decolorization was analyzed with pseudo-first-order (PFO) kinetic equation:

$$C_t = C_o e^{-k_{\text{obs}}^1 t} \quad (7)$$

where k_{obs}^1 is the observed rate constant (1/min).

2.3. Analysis

RGY concentration was analyzed by measuring the absorbance at 410 nm using a spectrophotometer (Thermo Scientific Evolution 201, USA). The concentration of Fe^{2+} in the solution was analyzed by measuring absorption at 510 nm using HACH FerroVer iron reagent® (HACH, USA). Chemical oxygen demand (COD) was determined using the Reactor Digestion Method HACH (Method 8000) with a HACH DR/3900 spectrophotometer. This method is USEPA approved for wastewater analyses (Standard Method 5220D) (APHA et al., 2012). COD digestion reagents were obtained from HACH Co. The American Dye Manufacturers Institute (ADMI) Tristimulus Filter Method was used for analyzing the true color of the solution (APHA et al., 2012). The ADMI value was determined under three preset wavelengths (438, 540, and 590 nm). In Taiwan, environmental regulations prescribe a discharge COD limit of 140 mg/L and a true color limit of ADMI 550 for wastewater from dyeing, printing, and textile industries.

3. Results and discussion

3.1. Decolorization of RGY in different comparable systems

Fig. 2a shows a comparison of different decolorization systems, including Fe^0 only, Fe^0 assisted with ultrasound (Fe^0/US), ultrasound-activated PS system (PS/US), PS/ Fe^0 , and PS/ Fe^0 assisted with ultrasound (PS/ Fe^0/US). The insignificant color removal in both Fe^0 only and Fe^0/US systems indicated that adsorption and reduction reactions between Fe^0 and RGY could be neglected. In the PS/US system, despite generating SO_4^- radicals (Eq. (4)) (Li et al., 2013) is possible, RGY decolorization efficiency was not effective compared to the PS/ Fe^0 system, which indicates only a small amount of SO_4^- was produced in the PS/US system.

Results of PS/US system also indicate that the RGY could not be oxidized by persulfate, even though persulfate is considered as a strong oxidant.

In the PS/ Fe^0 system, a notably decolorization efficiency (>90%) was achieved within 10 min. The release of sufficient

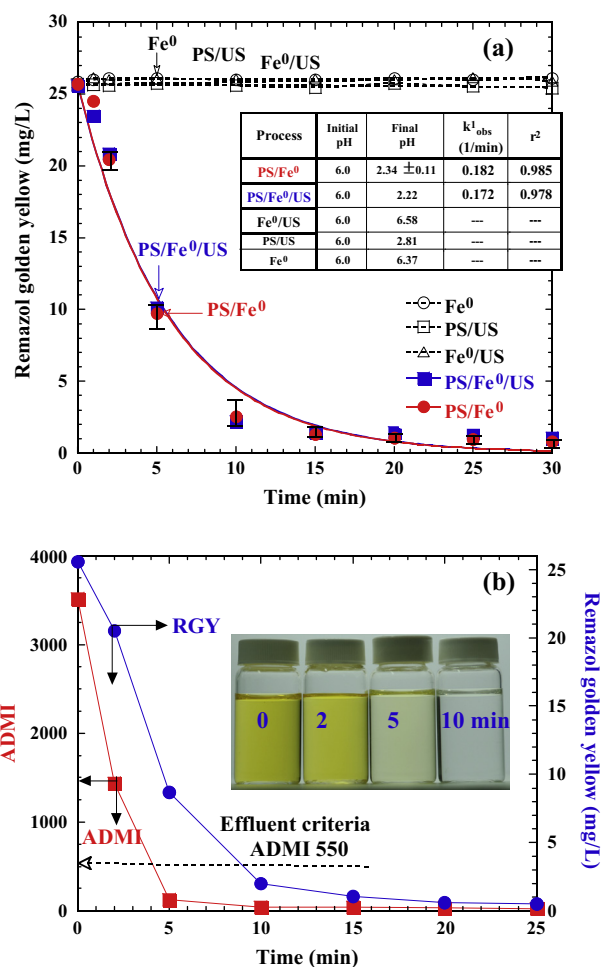
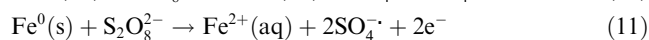
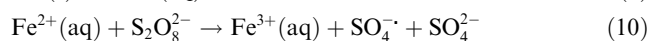
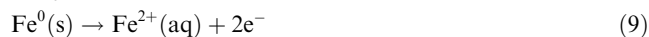
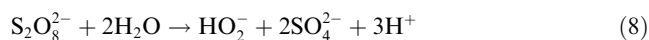


Figure 2 (a) Comparison of difference processes for RGY decolorization (initial pH 6.0, PS 5×10^{-3} M, Fe^0 0.5 g/L, US 120 W/L (10 min sonication)). Solid lines are the best fit of pseudo-first-order kinetics; (b) RGY, ADMI, and color depletion during the treatment of PS/ Fe^0 (PS 5×10^{-3} M, Fe^0 0.5 g/L, initial pH 6.0, 25 °C).

amount Fe^{2+} from Fe^0 aggregate is the key to generate $\text{SO}_4^{\cdot-}$ and decolor RGY effectively. In this system, the initial pH decreased from 6.0 to 2.32 (inset table in Fig. 2a) resulted from the hydrolysis of persulfate (Eq. (8)). Consequently, the corrosion of Fe^0 in acidic solution would produce Fe^{2+} (Eq. (9)). $\text{SO}_4^{\cdot-}$ radicals were produced as $\text{S}_2\text{O}_8^{2-}$ reacting with Fe^{2+} in the aqueous solution (Eq. (10)) (Fig. 3a) or directly contacting with Fe^0 surface (Eq. (11)) via surface heterogeneous reaction (Fig. 3b).



Ultrasonic irradiation not only enhanced corrosion of Fe^0 aggregate, but also produced more Fe^{2+} in the solution by refreshing the surface of Fe^0 (Eq. (12)) (Weng et al., 2014).



In the PS/ Fe^0 /US process, the addition of 10 min ultrasound could not further increase the decolorization efficiency. Study (Wang et al., 2014) showed that decolorization of Acid Orange 7 could be significantly enhanced by the introduction of ultrasound; our results indicated that such enhancement by ultrasound on PS/ Fe^0 is minimal. The different results can be ascribed to different dye types (acid vs. reactive) and Fe^0 forms (Fe^0 powder vs. Fe^0 aggregate) used in activating persulfate.

Fig. 2a shows that the RGY depletion by either PS/ Fe^0 or PS/ Fe^0 /US followed pseudo-first-order kinetics and the reaction could relate to fast homogeneous reaction occurring in the solution. The corresponding rate constant, k_{obs}^1 and regression coefficients (r^2) are shown in Fig. 2a (inset table). Because the value of k_{obs}^1 achieved in the Fe^0 /PS system was nearly the same in the Fe^0 /PS/US system, the introduction of ultrasound to the system is not necessary. The Fe^0 /PS process is a fast and effective process for RGY decolorization and is selected for further evaluation.

The photographs (Fig. 2b) show that the solution changed from yellow to light yellow after 5 min and then became transparent after 10 min of PS/ Fe^0 treatment. This indicated that the destruction of the chromophore structure ($-\text{N}=\text{N}-$ group) underwent persulfate oxidation easily. As shown, the true color decreased from ADMI 3519 to 124 within 5 min treatment, which complies with Taiwan's effluent criteria for true color (ADMI 550) in textile, paper, and dyeing industries.

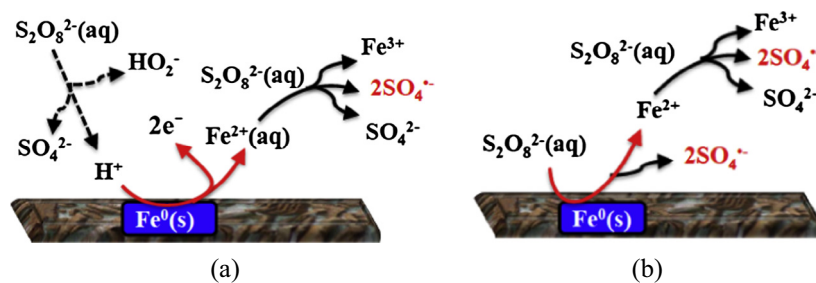


Figure 3 Conceptual reaction scheme of persulfate radicals generation via (a) aqueous homogeneous reaction and (b) surface heterogeneous reaction in the PS/ Fe^0 system.

3.2. Effect of pH

Solution pH is a crucial factor affecting the decolorization because pH governs the speciation of iron and solubility of Fe^0 aggregate. The effect of pH on RGY depletion in the PS/ Fe^0 system showed that a sharp depletion was observed at the initial pH between 4.0 and 10.0 (Fig. 4). At this pH region, satisfactory decolorization efficiency was achieved within 15 min of treatment. The depletion of dye and the variation of pH (inset graph in Fig. 4) were closely interrelated. When the initial pH was between 4.0 and 10.0, the solution pH decreased markedly to less than 3.0 within 5 min. In PS-driven oxidation reactions, the solution became sufficiently acid (Eq. (8)). The strongly acidic solution favors Fe^{2+} releasing from the corrosion of Fe^0 aggregate (Eq. (6)). The decolorization data at this pH range are well fitted by the PFO kinetics model with high regression coefficients (inset table in Fig. 4). The decolorization rate (k_{obs}^1) is proportionally correlated with a decrease in initial pH.

On the contrary, the solution pH remained nearly unchanged at an initial pH of 11.0, and insignificant dye depletion was observed. The insufficient of Fe^{2+} ion in the system would significantly hinder the activation of persulfate. Under basic conditions, although the generation of $\text{SO}_4^{\cdot-}$, superoxide radicals ($\text{O}_2^{\cdot-}$), and hydroxyl radicals ($\cdot\text{OH}$, $E^\circ = 2.70$ V) is possible (Eqs. (5) and (13)) (Liang et al., 2007; Furman et al., 2010), results show that RGY decolorization is ineffective at initial pH of 11.0.



3.3. Effect of persulfate concentration

Decolorization was also greatly enhanced by the increased addition of PS in the Fe^0 /PS system (Fig. 5a). The PFO rate law (Eq. (7)) applied well to the data within the reaction period (inset table in Fig. 5a). In general, RGY decolorization proceeded in a satisfactory manner for PS dosage higher than 2.5×10^{-3} M. However, the system with a low PS concentration (2×10^{-4} M) exhibited a slow reaction phenomenon. As the reaction proceeded, higher PS dosages led to lower the solution pH. The more acidic solution led to the release of greater amount of Fe^{2+} from the corrosion of Fe^0 (Fig. 5b). Thereby, more $\text{SO}_4^{\cdot-}$ radicals are produced for oxidizing RGY at a higher concentration of PS, which resulted in achieving a higher decolorization efficiency when sufficient Fe^{2+} was maintained in the system.

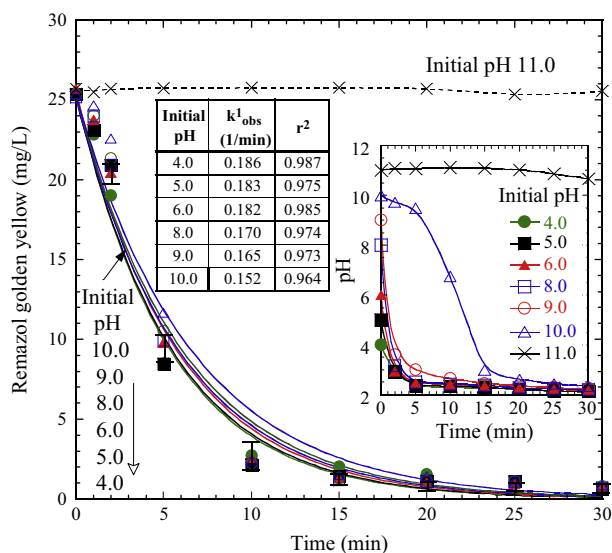


Figure 4 Effect of pH on RGY decolorization during the treatment of PS/ Fe^0 (PS 5×10^{-3} M, Fe^0 0.5 g/L, 25 °C). Solid lines are the best fits of pseudo-first-order kinetics.

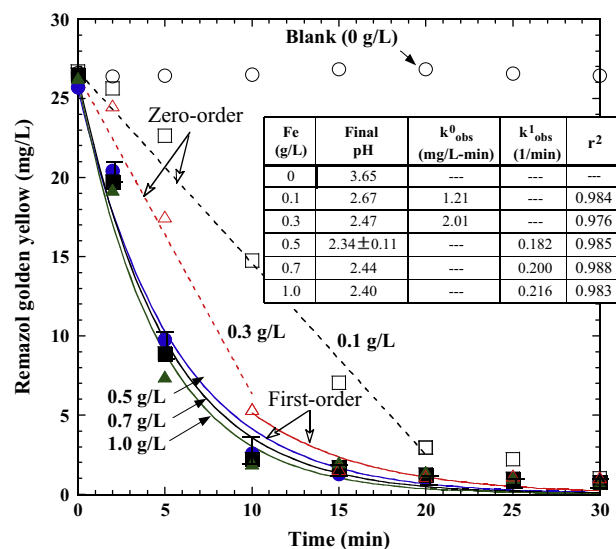


Figure 6 Effects of Fe^0 dosage on RGY decolorization during the treatment of PS/ Fe^0 (PS 5×10^{-3} M, initial pH 6.0, 25 °C). Dashed and solid lines are the best fits of zero-order kinetics and pseudo-first-order kinetics, respectively.

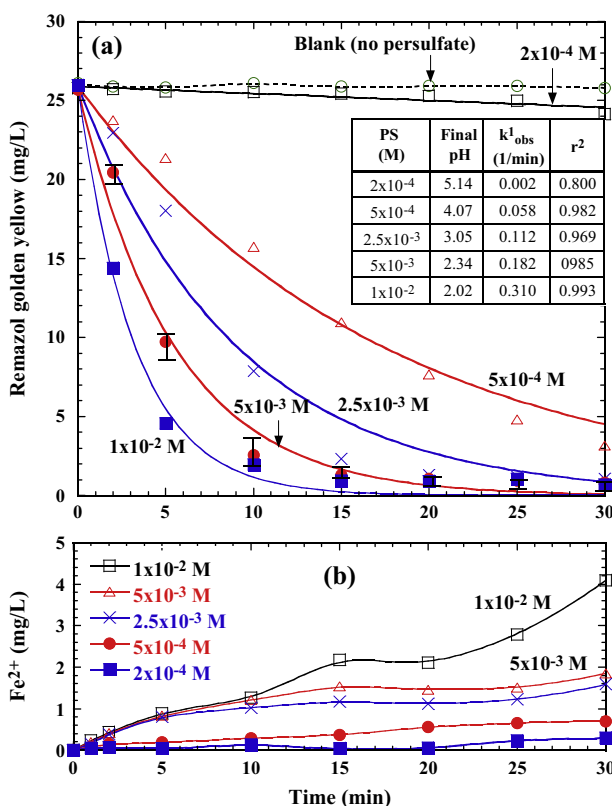


Figure 5 Effect of persulfate dosage on (a) RSY depletion and (b) variation of Fe^{2+} during the treatment of PS/ Fe^0 (Fe^0 0.5 g/L, initial pH 6.0, 25 °C). Solid lines in (a) are the best fits of pseudo-first-order kinetics.

3.4. Effect of Fe^0 dosages

Fig. 6 shows that decolorization was greatly enhanced by increasing the addition of Fe^0 in the Fe^0 /PS system. The

introduction of a higher Fe^0 dosage in the PS/ Fe^0 system resulted in higher decolorization efficiency. A fast decolorization efficiency (>90%) was achieved within 15 min for Fe^0 dosages higher than 0.5 g/L. However, system with low Fe^0 dosage (≤ 0.3 g/L) exhibited slow decolorization kinetics. Fast decolorization data are best described by the PFO kinetics model. As shown in the inset table in Fig. 6, the observed decolorization rate (k^1_{obs}) is proportionally correlated with an increase in the Fe^0 dosage. Increasing Fe^0 dosage led to the release of a greater amount of Fe^{2+} for catalyzing the persulfate reaction, which produced more $SO_4^{\cdot-}$ radicals to oxidize RGY and resulted in accelerating the decolorization rate. Slow decolorization data are well fitted by the zero-order rate law (Eq. (14)) and can be mostly attributed to the insufficient Fe^{2+} in the solution.

$$C_t = C_0 - k^0_{obs}t \quad (14)$$

where k^0_{obs} is the observed zero-order oxidation rate constant (mg/L min). The k^0_{obs} achieved in the system with Fe^0 dosage of 0.3 g/L and 0.1 g/L was 1.21 and 1.79 mg/L min, respectively (inset table in Fig. 6).

3.5. Effect of temperature on decolorization of RGY

Temperature plays a key role affecting RGY depletion for the PS and Fe^0 /PS systems. Although persulfate anions can be activated with thermal energy (Li et al., 2013; Deng et al., 2013) to generate sulfate radicals (Eq. (15)), RGY decolorization efficiency in the thermally activated persulfate system (PS/60 °C) is not promising (Fig. 7a).



When the PS was activated with Fe^0 at 60 °C (PS/ Fe^0 /60 °C), a prominent decolorization efficiency was achieved at an elevated temperature. As shown in Fig. 7a, RGY depletion increased proportionally with increasing

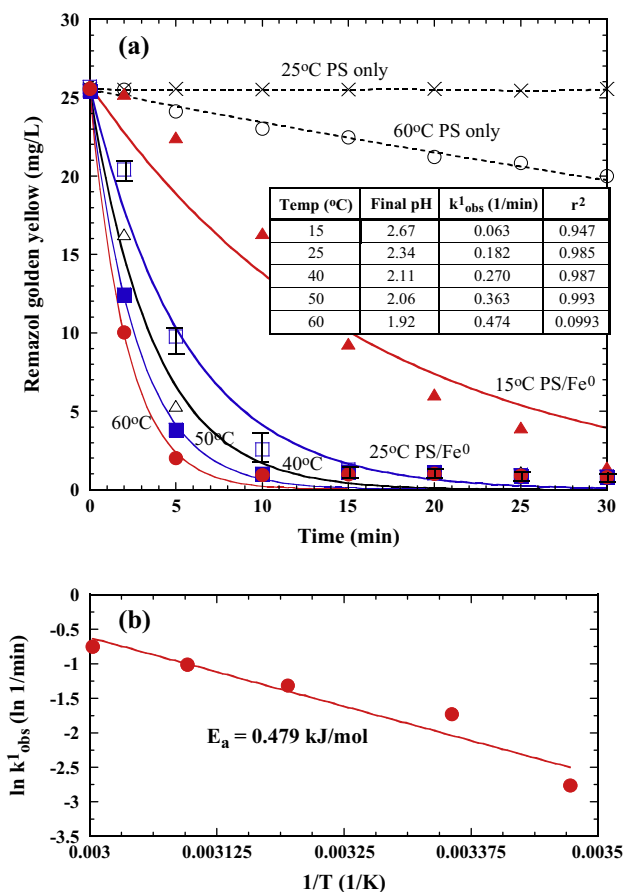


Figure 7 (a) Effect of temperature on RGY decolorization during the treatment of PS/Fe⁰ (PS 5×10^{-3} M, Fe⁰ 0.5 g/L, initial pH 6.0). Solid lines are the best fit of pseudo-first-order kinetics; (b) Arrhenius plots for the determination of activation energy of PS/Fe⁰ oxidation of RGY.

temperature from 15 °C to 60 °C. At higher temperatures, more energy is stored on the vibrational levels of the molecules, leading to an increase in molecular collision frequency, thereby accelerating the rate of decolorization. It appears that the catalytic activity of Fe⁰ aggregate remained high even the system was kept at elevated temperature of 60 °C.

Fig. 7a (inset table) shows the observed PFO rate constants (k_{obs}^1) for the PS only or PS/Fe⁰ processes. Based on the Arrhenius equation (Eq. (16)), the activation energy (E_a) of the PSs/Fe⁰ oxidation system was determined (Fig. 7b).

$$\ln k_{obs}^1 = (\ln A) - E_a/RT \quad (16)$$

where A = pre-exponential factor, E_a = the activation energy (kJ/mol), R = universal gas constant (1.987 cal/mol K), and T = absolute temperature (K). The E_a is 0.479 kJ/mol, which indicates the temperature dependence of RGY decolorization in the PS/Fe⁰ system is small.

3.6. Effect of salt

Effluents from textile and dyeing industries are often rich in color and contain variety of inorganic salts. The presence of high concentration salt is of great concern in the PS/Fe⁰

treatment process because it may influence the activity of oxidation reaction, thus affecting the dye degradation. Fig. 8a shows a negative effect of RGY decolorization in the PS/Fe⁰ system when the solution contained salts (NaClO₄, NaNO₃, NaCl, NaHCO₃, and Na₂HPO₄). The degree of decolorization behaved differently from the addition of these salts. The corresponding decolorization rate constants (k_{obs}^1) (inset table in Fig. 8a) are in decreasing order: no salt (0.182 1/min) > NaClO₄ (0.134 1/min) > NaNO₃ (0.110 1/min) > NaCl (0.087 1/min) > NaHCO₃ (0.016 1/min) > Na₂HPO₄ (0.007 1/min). At initial pH of 6.0, the dominant anion would be ClO₄⁻, NO₃⁻, Cl⁻, HCO₃⁻, H₂PO₄⁻, and HPO₄²⁻. The presence of HCO₃⁻ or Cl⁻ species in activated persulfate systems could increase the concentration of active radicals (HCO₃[•], CO₃^{•-}, Cl[•]) (Eqs. (17)–(20)) and possibly increase the oxidation efficiency of organic pollutants in wastewater (Yu et al., 2004; Bennedsen et al., 2012).

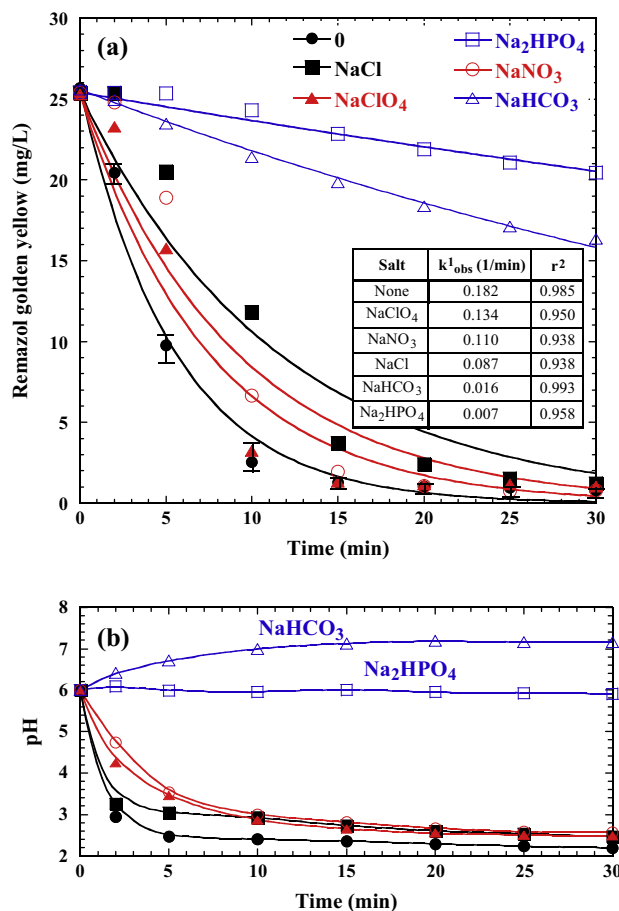
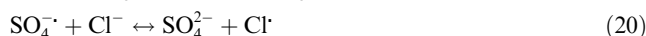
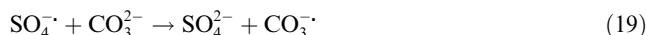
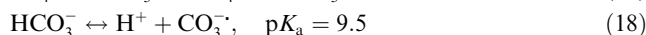


Figure 8 Effects of salt on RGY decolorization during the treatment of PS/Fe⁰ (PS 5×10^{-3} M, Fe⁰ 0.5 g/L, initial pH 6.0, all salts 5×10^{-3} M, 25 °C). (a) RGY depletion, (b) variation of pHs. Solid lines are the best fit of pseudo-first-order kinetics.

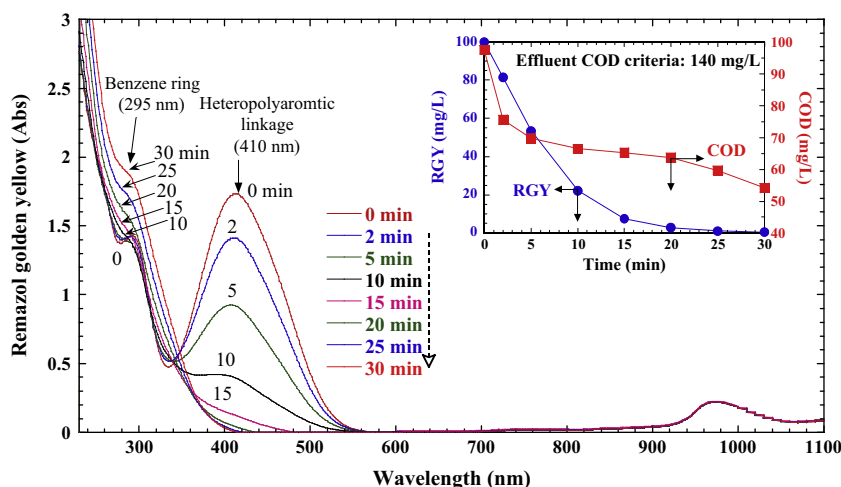


Figure 9 The variation of UV-vis spectra during the depletion of RGY in the PS/Fe⁰ system (RGY 100 mg/L, PS 5×10^{-3} M, Fe⁰ 0.5 g/L, initial pH 6.0, 25 °C). The graph insets are the COD, ADMI, and color depletion during the treatment.

However, inhibitory effect has been reported in a cobalt activated PS system for decolorization of Acid Orange 7 (Yuan et al., 2011) as solution contained concentration of NaCl less than 0.4 M; only hyper-concentration of NaCl (0.5 M) could enhance bleaching rate and NaCl higher than 5×10^{-3} M could decrease the inhibitory effect. Wang et al. (2011) have also found that Cl⁻ exhibited a significant inhibiting effect at low concentration (≤ 0.01 mol/L) in Co²⁺ activated peroxymonosulfate system for decolorization of Acid Orange 7. Our results clearly indicated that the dye oxidation was suppressed by the presence of these anions. The inhabitation of dye oxidation on the PS/Fe⁰ system was possible due to Cl⁻ served as SO₄⁻ radicals scavengers to form less reactive less Cl⁻ radicals (Eq. (20)) (Yuan et al., 2011). The adverse effects of dye oxidation were by Cl⁻, NO₃⁻, and NaClO₄⁻, and could also attributed to the fact that high concentration of salts would disturb the oxidation reaction due to the electronic interference resulted from the high ionic concentration (Weng et al., 2013), thereby decreasing the rate of decolorization. Particularly, the rate of RGY decolorization was inhibited significantly by the presence of NaHCO₃ and Na₂HPO₄. Such effect is closely related to the pH variation during the treatment period (Fig. 8b). The pH was keeping at near neutral in the system containing NaHCO₃ or Na₂HPO₄, which limited the corrosion of Fe⁰ aggregate. The formation of Fe(H₂PO₄)₃ and Fe(HCO₃)₃ under neutral pH condition is more stable than the complexes formed by NO₃⁻, ClO₄⁻, and Cl⁻. The complexation formation also greatly affects the availability of Fe²⁺ and Fe³⁺ ions in the persulfate oxidation (Eqs. (9)–(11)) to generate SO₄⁻ for RGY decolorization. Because the ionic strength of Na₂HPO₄ (ca. as 1.5×10^{-2} M) is higher than that of NaHCO₃ (ca. as 5×10^{-3} M) for a system with same salt concentration (5×10^{-3} M), the interference effect on the reactivity of persulfate reaction is higher. Consequently, decolorization rate was lower in the PS/Fe⁰ system containing Na₂HPO₄ and NaHCO₃.

3.7. Decolorization mechanisms

To relate the changes in chemical structure of RGY and color depletion during PS/Fe⁰ treatment, the UV-vis spectra, dye

concentration, and COD were measured during the treatment (Fig. 9). For an initial RGY concentration of 100 mg/L, approximately 98% decolorization efficiency was achieved within 20 min (inset graph in Fig. 9). Before the reaction, the spectra of RGY were characterized by one main band in the visible region with absorbance peak at 410 nm and a narrow absorbance peak at 295 nm in the ultraviolet region. After the reaction, the characteristic peak decreased quickly within 15 min and the peaks reduced to the minimum. This implies that the conjugate chromophore structure (–N=N– group) of RGY was destroyed and the color disappeared rapidly. Additionally, the increase of the absorbance with time at 295 nm was the evidence of the appearance of aromatic fragments as the reaction proceeded after breaking down RGY chromophore group.

A prominent COD removal was observed within 5 min reaction, indicating that RGY is easily oxidized by PS/Fe⁰ (inset graph in Fig. 9). A 55.6% of residual COD was found

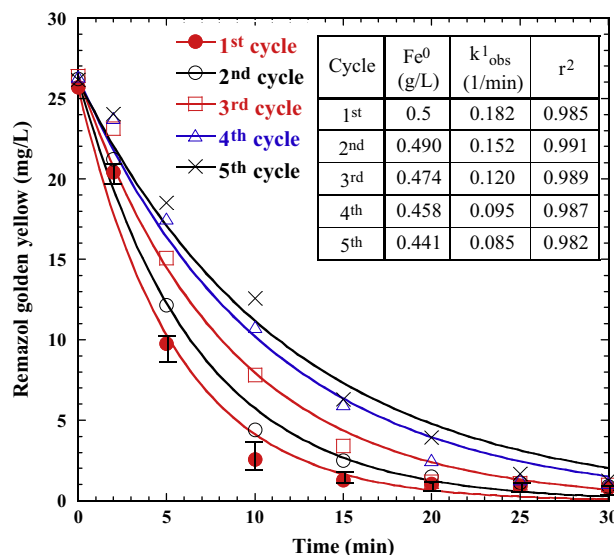


Figure 10 Effect of recycled Fe⁰ aggregate on RGY decolorization in the PS/Fe⁰ system (PS 5×10^{-3} M, initial pH 6.0, 25 °C).

even though the color was completely disappeared within 30 min, which indicates all RGY in this process was not completely oxidized into carbon dioxide. The residual COD was mainly attributed to the formation of intermediate products of RGY, such as benzene, phenol, and carboxylic acids. The COD value decreased from the initial value of 97.5 to 54.2 mg/L, which was far below Taiwan's discharge criterion (140 mg/L) for textile and dyeing industries.

The possible degradation pathway in the PS/Fe⁰ system for oxidation of RGY is proposed. SO₄^{-•} radicals could remove electrons from RGY. When SO₄^{-•} radicals added to the azo bonds, the azo bonds cleaved to form azobenzene. Azobenzene was oxidized by SO₄^{-•} radicals to form phenol and benzene. SO₄^{-•} could further attack on benzene ring because it is an electrophilic radical (Liang et al., 2008). Then phenol was further oxidized to hydroquinone and benzo-1,4-quinone. Benzene ring was cleaved to produce but-2-enedioic acid and then finally oxidized to carboxylic acids. Carboxylic acids, such as formic acid and acetic acid, are more difficult to be oxidized than their parent compounds (Ramirez et al., 2005; Wang et al., 2014; Weng and Huang, 2015). To improve COD removal, prolonging reaction time or employing more aggressive operating conditions, such as PS/Fe⁰ in conjunction with ultrasound/heat, could be considered in further study.

3.8. Reusability of Fe⁰ aggregate

The reusability of the Fe⁰ aggregate in the PS/Fe⁰ system is crucial for its practical application. The Fe⁰ was separated from the reaction mixture at the end of each cycle. Fig. 10 shows the performance of using recycled Fe⁰ aggregate in the PS/Fe⁰ system for five consecutive cycles. The mass of Fe⁰ decreased gradually from 0.5 g/L in the 1st cycle to 0.441 g/L after the 5th cycle. Based on a unit price of Fe⁰ aggregate (500 USD/ton), the average cost of Fe⁰ is only 5.9 × 10⁻³ USD/m³ for each cycle. The RGY decolorization efficiency and the rate of decolorization (*k*_{obs}¹) are inversely proportional to the number of times Fe⁰ aggregate is recycled due to the gradual loss of Fe⁰ activity and the mass of Fe. Although a negative effect resulted from using the recycled Fe⁰ aggregate, decolorization occurred quickly without any delay of oxidation even when Fe⁰ aggregate was repeatedly used for five consecutive cycles. Because of its fast and effective azo-dye removal, and reusability, the Fe⁰ aggregate has potential applications in the PS/Fe⁰ system for dye laden wastewater treatment.

4. Conclusions

Persulfate oxidation activated by Fe⁰ aggregate for decolorization of reactive azo dye provides an effective technology for decolorization of Remazol Golden Yellow. Decolorization by PS/Fe⁰ process was favorable at initial pH < 10.0, high Fe⁰ and persulfate dosages, and high temperature. However, the rate of RGY decolorization was inhibited significantly by the addition of NaHCO₃ and Na₂HPO₄. Further study may focus on minimizing such inhibitory effect by the addition of ultrasound or heat to the process. The Fe⁰ aggregate has advantages of low-cost (500 USD/ton), effective decolorization, reusability, and ease of operation (easy to be separated

after use), which shows the practically feasible of Fe⁰ aggregate as an economic and efficient activator for the persulfate oxidation of reactive azo dye.

Acknowledgments

Financial support by the Ministry of Science and Technology, Taiwan (Grant No. NSC102-2221-E214-002-MY3) and the Fe⁰ aggregate samples provided from Connelly-GPM Inc., USA, are gratefully acknowledged.

References

- Al-Shamsi, A.M., Thomson, N.R., 2013. Treatment of organic compounds by activated persulfate using nanoscale zero valent iron. *Ind. Eng. Chem. Res.* 52, 13564–13571.
- Alvarenga, J.M., Fideles, R.A., Silva, M.V., Murari, G.F., Taylor, J.G., Lemos, L.R., Rodrigues, G.D., Mageste, A.B., 2015. Partition study of textile dye Remazol yellow gold RNL in aqueous two-phase systems. *Fluid Phase Equilib.* 391, 1–8.
- APHA, AWWA, WEF, 2012. Standard Methods for the Examination of Water and Wastewater, 22nd ed.. American Public Health Association, Washington, DC, USA.
- Benndesen, L.R., Muff, J., Søgaard, E.G., 2012. Influence of chloride and carbonates on the reactivity of activated persulfate. *Chemosphere* 86, 1092–1097.
- Cai, C., Wang, L., Gao, H., Hou, L., Zhang, H., 2014. Ultrasound enhanced heterogeneous activation of peroxydisulfate by bimetallic Fe-Co/GAC catalyst for the degradation of acid orange 7 in water. *J. Environ. Sci.* 26, 1267–1273.
- Deng, J., Shao, Y., Gao, N., Deng, Y., Zhou, S., Hu, X., 2013. Thermally activated persulfate (TAP) oxidation of antiepileptic drug carbamazepine in water. *Chem. Eng. J.* 228, 765–771.
- Fang, G.D., Dionysiou, D.D., Al-Abed, S.R., Zhou, D.M., 2013. Superoxide radical driving the activation of persulfate by magnetite nanoparticles: implications for the degradation of PCBs. *Appl. Catal. B: Environ.* 129, 325–332.
- Furman, O.S., Teel, A.L., Watts, R.J., 2010. Mechanism of base activation of persulfate. *Environ. Sci. Technol.* 44, 6423–6428.
- Han, D., Wan, J., Ma, Y., Wang, Y., Huang, M., Chen, Y., Li, D., Guan, Z., Li, Y., 2014. Enhanced decolorization of orange G in a Fe(II)-EDDS activated persulfate process by accelerating the regeneration of ferrous iron with hydroxylamine. *Chem. Eng. J.* 256, 316–323.
- Hemapriyamvadhya, R., Sivasankar, T., 2015. Sonophotocatalytic treatment of methyl orange dye and real textile effluent using synthesised nano-zinc oxide. *Color. Technol.* 131, 110–119.
- Ji, Y., Dong, C., Kong, D., Lu, J., Zhou, Q., 2015. Heat-activated persulfate oxidation of atrazine: implications for remediation of groundwater contaminated by herbicides. *Chem. Eng. J.* 263, 45–54.
- Jo, Y.H., Do, S.H., Kong, S.H., 2014. Persulfate activation by iron oxide-immobilized MnO₂ composite: identification of iron oxide and the optimum pH for degradations. *Chemosphere* 95, 550–555.
- Kobya, M., Can, O.T., Bayramoglu, M., 2003. Treatment of textile wastewaters by electrocoagulation using iron and aluminum electrodes. *J. Hazard. Mater.* B100, 163–178.
- Lee, Y.C., Lo, S.L., Kuo, J., Huang, C.P., 2013. Promoted degradation of perfluorooctanoic acid by persulfate when adding activated carbon. *J. Hazard. Mater.* 261, 463–469.
- Li, B., Li, L., Lin, K., Zhang, W., Lu, S., Luo, Q., 2013. Removal of 1,1,1-trichloroethane from aqueous solution by a sono-activated persulfate process. *Ultrason. Sonochem.* 20, 855–863.
- Li, H., Wan, J., Ma, Y., Wang, Y., Huang, M., 2014a. Influence of particle size of zero-valent iron and dissolved silica on the reactivity

- of activated persulfate for degradation of acid orange 7. *Chem. Eng. J.* 237, 487–496.
- Li, H., Wan, J., Ma, Y., Huang, M., Wang, Y., Chen, Y., 2014b. New insights into the role of zero-valent iron surface oxidation layers in persulfate oxidation of dibutyl phthalate solutions. *Chem. Eng. J.* 250, 137–147.
- Liang, C.J., Lai, M.C., 2008. Trichloroethylene degradation by zero valent iron activated persulfate oxidation. *Environ. Eng. Sci.* 25, 1071–1077.
- Liang, C.J., Wang, Z.S., Bruel, C.J., 2007. Influence of pH on peroxydisulfate oxidation of TCE at ambient temperatures. *Chemosphere* 66, 106–113.
- Liang, C., Huang, C.F., Chen, Y.J., 2008. Potential for activated persulfate degradation of BTEX contamination. *Water Res.* 42, 4091–4100.
- Lin, H., Wu, J., Zhang, H., 2013. Degradation of bisphenol a in aqueous solution by a novel electro/ Fe^{3+} /peroxydisulfate process. *Sep. Purif. Technol.* 117, 18–23.
- Long, A.H., Lei, Y., Zhang, H., 2014. Degradation of toluene by a selective ferrous ion activated persulfate oxidation process. *Ind. Eng. Chem. Res.* 53, 1033–1039.
- Oh, S.Y., Kang, S.G., Chiu, P.C., 2010. Degradation of 2,4-dinitrotoluene by persulfate activated with zero-valent iron. *Sci. Total Environ.* 408, 3464–3468.
- Ozbay, N., Yargic, A.S., 2015. Factorial experimental design for Remazol yellow dye sorption using apple pulp/apple pulp carbon/titanium dioxide co-sorbent. *J. Cleaner Prod.* <http://dx.doi.org/10.1016/j.jclepro.2015.03.050>.
- Pei, Y., Wang, M., Tian, D., Xu, X., Yuan, L., 2015. Synthesis of core-shell SiO_2 @MgO with flower like morphology for removal of crystal violet in water. *J. Colloid Interface Sci.* <http://dx.doi.org/10.1016/j.jcis.2015.05.003>.
- Pukdee-Asa, M., Su, C.C., Ratanatamskul, C., Lu, M.C., 2011. Degradation of azo dye by the fluidized-bed Fenton process. *Color. Technol.* 128, 28–35.
- Ramirez, J.H., Costa, C.A., Madeira, L.M., 2005. Experimental design to optimize the degradation of the synthetic dye Orange II using Fenton's reagent. *Catal. Today* 107–108, 68–76.
- Rasalingam, S., Peng, R., Koodali, R.T., 2015. An insight into the adsorption and photocatalytic degradation of rhodamine B in periodic mesoporous materials. *Appl. Catal. B: Environ.* 174–175, 49–59.
- Raschitor, A., Fernandez, C.M., Cretescua, I., Rodrigo, M.A., Cañizares, P., 2014. Sono-electrocoagulation of wastewater polluted with Rhodamine 6G. *Sep. Purif. Technol.* 135, 110–116.
- Rodriguez, S., Vasquez, L., Costa, D., Romero, A., Santos, A., 2014. Oxidation of orange G by persulfate activated by Fe(II), Fe(III) and zero valent iron (ZVI). *Chemosphere* 101, 86–92.
- Shi, Q., Li, A., Qing, Z., Li, Y., 2015. Oxidative degradation of orange G by persulfate activated with iron-immobilized resin chars. *J. Ind. Eng. Chem.* <http://dx.doi.org/10.1016/j.jiec.2014.11.010>.
- Somasekhara Reddy, M.C., Nirmala, 2014. Bengal gram seed husk as an adsorbent for the removal of dyes from aqueous solutions – column studies. *Arab. J. Chem.* <http://dx.doi.org/10.1016/j.arabj.2014.08.026>.
- Su, S.N., Guo, W.L., Leng, Y.Q., Yi, C.L., Ma, Z.M., 2013. Heterogeneous activation of oxone by $\text{Co}_x\text{Fe}_{3-x}\text{O}_4$ nanocatalysts for degradation of rhodamine B. *J. Hazard. Mater.* 244, 736–742.
- Wang, P., Yang, S., Shan, L., Niu, R., Shao, X., 2011. Involvements of chloride ion in decolorization of acid orange 7 by activated peroxydisulfate or peroxymonosulfate oxidation. *J. Environ. Sci.* 23, 1799–1807.
- Wang, X., Wang, L., Li, J., Qiu, J., Cai, C., Zhang, H., 2014. Degradation of acid orange 7 by persulfate activated with zero valent iron in the presence of ultrasonic irradiation. *Sep. Purif. Technol.* 122, 41–46.
- Weng, C.H., Huang, V., 2015. Application of Fe^0 aggregate in ultrasound enhanced advanced Fenton process for decolorization of methylene blue. *J. Ind. Eng. Chem.* 28, 153–160.
- Weng, C.H., Lin, Y.T., Lin, T.Y., Kao, C.M., 2007. Enhancement of electrokinetic remediation of hyper-Cr(VI) contaminated clay by zero-valent iron. *J. Hazard. Mater.* 149, 292–302.
- Weng, C.H., Lin, Y.T., Yuan, H.M., 2013. Rapid decoloration of reactive black 5 by an advanced Fenton process in conjunction with ultrasound. *Sep. Purif. Technol.* 117, 75–82.
- Weng, C.H., Lin, Y.T., Liu, N., Yang, H.Y., 2014. Enhancement of advanced Fenton process ($\text{Fe}^0/\text{H}_2\text{O}_2$) by ultrasound for decolorization of real textile wastewater. *Color. Technol.* 130, 133–139.
- Wilkin, R.T., Su, C., Ford, R.G., Paul, C.J., 2005. Chromium removal processes during groundwater remediation by a zero valent iron permeable reactive barrier. *Environ. Sci. Technol.* 39, 4599–4605.
- Xie, X.F., Zhang, Y.Q., Huang, W.L., Huang, S.B., 2012. Degradation kinetics and mechanism of aniline by heat-assisted persulfate oxidation. *J. Environ. Sci.* 24, 821–826.
- Xing, T., Kai, H., Chen, G., 2012. Study of adsorption and desorption performance of acid dyes on anion exchange membrane. *Color. Technol.* 131, 110–119.
- Yan, J., Han, L., Gao, W., Xue, S., Chen, M., 2015. Biochar supported nanoscale zerovalent iron composite used as persulfate activator for removing trichloroethylene. *Bioresour. Technol.* 175, 269–274.
- Yang, S.Y., Wang, P., Yang, X., Wei, G., Zhang, W.Y., Shan, L., 2009. A novel advanced oxidation process to degrade organic pollutants in wastewater: microwave-activated persulfate oxidation. *J. Environ. Sci.* 21, 1175–1180.
- Yang, S.Y., Yang, X., Shao, X.T., Niu, R., Wang, L.L., 2011. Activated carbon catalyzed persulfate oxidation of azo dye acid orange 7 at ambient temperature. *J. Hazard. Mater.* 186, 659–666.
- Yu, X.Y., Bao, Z.C., Barker, J.R., 2004. Free radical reactions involving Cl^+ , Cl_2^+ , and SO_4^+ in the 248 nm photolysis of aqueous solutions containing $\text{S}_2\text{O}_8^{2-}$ and Cl^- . *J. Phys. Chem. A* 108, 295–308.
- Yuan, R., Ramjaun, S.N., Wang, Z., Liu, J., 2011. Effects of chloride ion on degradation of acid orange 7 by sulfate radical-based advanced oxidation process: implications for formation of chlorinated aromatic compounds. *J. Hazard. Mater.* 196, 173–179.
- Yuan, Y., Hong Tao, H., Fanb, J., Ma, L., 2015. Degradation of p-chloroaniline by persulfate activated with ferrous sulfide ore particles. *Chem. Eng. J.* 268, 38–46.
- Zhao, Y.S., Sun, C., Sun, J.Q., Zhou, R., 2015. Kinetic modeling and efficiency of sulfate radical-based oxidation to remove p-nitroaniline from wastewater by persulfate/ Fe_3O_4 nanoparticles process. *Sep. Purif. Technol.* 142, 182–188.
- Zhou, X., Wang, Q., Jiang, G., Liu, P., Yuan, Z., 2015. A novel conditioning process for enhancing dewaterability of waste activated sludge by combination of zero-valent iron and persulfate. *Bioresour. Technol.* 185, 416–420.
- Zhu, L., Ai, Z., Ho, W., Zhang, L., 2013. Core-shell $\text{Fe}-\text{Fe}_2\text{O}_3$ nanostructures as effective persulfate activator for degradation of methyl orange. *Sep. Purif. Technol.* 108, 159–165.